



Revisiting the nature and pharmacodynamics of tacrolimus metabolites

Rudy Mevizou^{a,b,1}, Hassan Aouad^{a,1}, François-Ludovic Sauvage^a, H el ene Arnion^a,
Emilie Pinault^{a,c}, Jean-S ebastien Bernard^a, Gildas Bertho^d, Nicolas Giraud^d,
Rodolphe Alves de Sousa^d, Adolfo Lopez-Noriega^b, Florent Di Meo^{a,c}, M elanie Campana^b,
Pierre Marquet^{a,e,*}

^a Universit e de Limoges, Inserm, UMR1248, Pharmacology & Transplantation P&T, Limoges, France

^b Medincell, Jacou, France

^c Universit e de Limoges, CNRS, Inserm, CHU Limoges, UAR2015, US42, Integrative Biology Health Chemistry and Environment BISCEm, Limoges, France

^d Universit e Paris Cit e, CNRS, Laboratoire de Chimie et de Biochimie Pharmacologiques et Toxicologiques, Paris, France

^e Department of Pharmacology, Toxicology and Pharmacovigilance, Centre Hospitalier Universitaire de Limoges, Limoges, France

ARTICLE INFO

Keywords:

Tacrolimus
Metabolites
Structures
Pharmacodynamics
Pharmacodynamic interactions

ABSTRACT

The toxicity of tacrolimus metabolites and their potential pharmacodynamic (PD) interactions with tacrolimus might respectively explain the surprising combination of higher toxicity and lower efficacy of tacrolimus despite normal blood concentrations, described in extensive metabolizers. To evaluate such interactions, we produced tacrolimus metabolites *in vitro* and characterized them by high resolution mass spectrometry (HRMS, for all) and nuclear magnetic resonance (NMR, for the most abundant, M-I). We quantified tacrolimus metabolites and checked their structure in patient whole blood and peripheral blood mononuclear cells (PBMC). We explored the interactions of M-I with tacrolimus *in silico*, *in vitro* and *ex vivo*. *In vitro* metabolization produced isoforms of tacrolimus and of its metabolites M-I and M-III, whose HRMS fragmentation suggested an open-ring structure. M-I and M-III open-ring isomers were also observed in patient blood. By contrast, NMR could not detect these open-ring forms. Transplant patients expressing CYP3A5 exhibited higher M-I/TAC ratios in blood and PBMC than non-expressers. Molecular Dynamics simulations showed that: all possible tacrolimus metabolites and isomers bind FKBP12; and the hypothetical open-ring structures induce looser binding between FKBP12 and calcineurins, leading to lower CN inhibition. *In vitro*, tacrolimus bound FKBP12 with more affinity than purified M-I, and the pool of tacrolimus metabolites and purified M-I had only weak inhibitory activity on IL2 secretion and not at all on NFAT nuclear translocation. M-I showed no competitive effect with tacrolimus on either test. Finally, M-I or the metabolite pool did not significantly interact with tacrolimus MLR suppression, thus eliminating a pharmacodynamic interaction.

1. Introduction

Organ transplantation is currently the best treatment option for solid organ failure (*i.e.* kidneys, heart, liver or lungs), but it requires life-long immune-suppressive therapy to prevent allograft rejection and loss-of-

function. Tacrolimus (initially coded as FK506), a calcineurin inhibitor (CNI), is part of a vast majority of immunosuppressive regimens in solid organ transplantation. This 23-membered macrolide, isolated from *Streptomyces tsukubensis* in the late 1980's, has rapidly supplanted cyclosporine, the first CNI used in organ transplantation [1], due to its

Abbreviations: BBH, Calcineurin B Binding Helix; CI95 %, 95 % confidence interval; CN, Calcineurin; CNI, Calcineurin inhibitor; DFT, Density Functional Theory; EPI, Enhanced Product Ion; FK506, Tacrolimus; FKBP12, 12 kDa FK506 Binding Protein; HLM, Human Liver Microsomes; HMBC, Heteronuclear Multiple Bond Correlation; HRMS, High Resolution Mass Spectrometry; MD, Molecular Dynamics; MLR, Mixed Lymphocyte Reaction; MRM-HR, High Resolution Mass Spectrometry in the Multiple Reaction Monitoring; MS, Mass spectrometry; NFAT, Nuclear Factor of Activated T-cells; NMR, Nuclear Magnetic Resonance; PBMC, Peripheral Blood Mononuclear Cells; PD, Pharmacodynamics; PDB, Protein Data Bank; PMA, Phorbol Myristate Acetate; RMSD, Root-Mean Squared Deviation; STD, Standard Deviation.

* Correspondence to: Department of Pharmacology, Toxicology and Pharmacovigilance, CHU Limoges, 2 avenue Martin Luther King, Limoges 87000, France.

E-mail address: pierre.marquet@unilim.fr (P. Marquet).

¹ These authors contributed equally.

<https://doi.org/10.1016/j.yphrs.2024.107438>

Received 6 September 2024; Received in revised form 27 September 2024; Accepted 27 September 2024

Available online 30 September 2024

1043-6618/  2024 The Author(s). Published by Elsevier Ltd. This is an open access article under the CC BY license (<http://creativecommons.org/licenses/by/4.0/>).

better benefit-risk balance [2,3].

Tacrolimus dosing is complicated by a narrow therapeutic window and high inter- and intra-patient pharmacokinetic variability, which places patients at risk of underexposure and allograft rejection or overexposure and toxicity. Even today, the origins of the variability in the therapeutic efficacy and toxicity of tacrolimus are not fully elucidated. Although a vast majority of drug metabolites are in general pharmacologically inactive, some of them can be significantly or entirely responsible for the therapeutic effect of a drug. To the best of our knowledge, the hypothesis that metabolites can decrease or even reverse the pharmacological action of the parent drug has very seldom been explored up until now.

Tacrolimus is extensively metabolized by CYP3A5 and CYP3A4 isoenzymes in the intestine and the liver, with CYP3A4 having a lower efficiency for catalysis. In the 90's, it was reported that up to fifteen metabolites may be formed by demethylation, hydroxylation or combinations of both [4]. Among them, eight metabolites classified as first- and second-generation metabolites were produced by incubating tacrolimus with rat liver microsomes and characterized using NMR [5, 6]. Five of these metabolites (desmethyl-, didesmethyl-, hydroxy-, desmethyl-hydroxy- and didesmethyl-hydroxy- tacrolimus) were further detected with LC-MS [7–9] in transplant patients' blood, bile and urine. The major metabolite was reported to be 13-O-desmethyl-tacrolimus (M-I), while 31-O-desmethyl-tacrolimus (M-II) and 15-O-desmethyl-tacrolimus (M-III) were hardly detectable [10,11].

The role of these metabolites in tacrolimus efficacy and toxicity has not yet been investigated thoroughly and is probably underestimated. *In vitro* studies from 30 years ago showed that: (i) M-I binds FKBP12 with 10-fold less affinity than tacrolimus, leading to pentamer complex formation with calcineurins A and B and calmodulin, with 13 % of tacrolimus efficacy, and exhibits 6.4 % of tacrolimus mixed lymphocyte reaction (MLR) suppression; (ii) M-II binds FKBP12 with lower affinity too, but exhibits pentamer formation and MLR suppression similar to those of tacrolimus [12]; and (iii) M-III (15-O-desmethyl-tacrolimus) binds FKBP12 with slightly more affinity than tacrolimus but is not able to form a pentamer, or to suppress MLR [12]. This suggests that tacrolimus metabolites, in particular M-I and M-III, might at least partially inhibit tacrolimus efficacy through competitive FKBP binding and/or pentamer formation. In the clinics, statistical associations between the blood levels of these metabolites, polymorphisms of the cytochromes and membrane transporters, and tacrolimus related toxicity, have been reported in small patient groups. Polymorphisms in the *CYP3A5* and *ABCB1* genes were associated with neurotoxicity in tacrolimus treated stem cell patients [13], suggesting that both the blood-brain barrier permeability and tacrolimus metabolites may be involved. M-III (but not M-I) blood levels were associated with the estimated glomerular filtration rate, red blood cell count and infections in kidney transplant recipients [14]. Later on, the same team reported a positive correlation of the M-I/tacrolimus ratio with alanine aminotransferase levels, suggesting either accumulation in liver dysfunction or hepatotoxicity of M-I, and a negative correlation with hemoglobin, maybe due to lower tacrolimus whole blood levels in anemia or myelotoxicity [15]. Finally, metabolite toxicity, and pharmacodynamic interactions between tacrolimus and its metabolites, might respectively explain the surprising combination of higher toxicity and lower efficacy of tacrolimus in extensive metabolizers, despite “normal” tacrolimus blood concentration [16]. However, such pharmacodynamic interactions have never been tested.

As a first step into the elucidation of the role of tacrolimus metabolites in the drug benefit-risk balance, the aim of this study was to evaluate the pharmacodynamic interactions of the main tacrolimus metabolites with the parent drug, through the combination of modern technologies. To this effect: (i) we produced and characterized tacrolimus metabolites, and purified M-I, the most abundant one; (ii) we quantified tacrolimus metabolites and checked their structure in patient whole blood and PBMC; and (iii) we studied the pharmacodynamics of

M-I and its pharmacodynamic interactions with tacrolimus, *in silico*, *in vitro* and *ex vivo*.

2. Patients and methods

Detailed methods are available as [Supplementary material](#) and methods.

2.1. Production, purification and quantitation of tacrolimus and metabolites

2.1.1. High resolution mass spectrometry characterization

Tacrolimus metabolites were produced by incubating tacrolimus with human liver microsomes (HLM) *in vitro*. As a first step of structure elucidation, their fragmentation spectra by micro-HPLC – high resolution mass spectrometry (HRMS) on a TripleTOF® 5600+ instrument (Sciex, France) were compared with that of tacrolimus in a systematic, stepwise manner. After *in silico* mass fragmentation of tacrolimus using Mass Frontier™ 8.0 (Thermo Scientific), the theoretical mass of each fragment was compared with the mean fragment masses observed to determine their most likely structural formula.

2.1.2. NMR analysis of tacrolimus M-I metabolite

For further elucidation of the structure of the major M-I metabolite by NMR, tacrolimus was metabolized in large amounts by S9 fractions prepared from the liver of a conventional 6-week-old pig. The incubation medium was freeze-dried and the residue resuspended and back-extracted in acetonitrile twice. The organic phase was dried and the metabolites were finally extracted using Oasis® HLB 3 mL 60 mg cartridges and methanol. The methanol phase was purified using directed fractionation on a Thermo LC preparative system. The fractions containing M-I were freeze-dried to obtain a powder, which was purified again in the same conditions, after solubilization of the powder in methanol. The fractions obtained were controlled by LC-MS/MS using a Prominence/8060NX instrument (Shimadzu, France), following three MRM transitions for M-I: 812.4 > 602.3; 812.4 > 491.2 and 812.4 > 345.2.

Commercial tacrolimus and purified M-I were dissolved with CDCl₃ at 0.6 g/L. NMR experiments were carried out at 300 K on a spectrometer operating at 500.45 MHz for ¹H, equipped with a cryogenic 5 mm ¹³C/¹H dual probe containing z-gradient axis. One-dimension (1D) ¹H spectra and ¹³C spectra were acquired. 2D homonuclear ¹H-¹H COSY and ¹H-¹H TOCSY spectra and 2D ¹H-¹³C edited-HSQC and ¹H-¹³C heteronuclear multiple bond correlation (HMBC) spectra were recorded on samples at natural ¹³C abundance.

2.2. Structure and concentrations of tacrolimus metabolites in patient blood and PBMC

Patient blood samples were collected and kept in an accredited local biobank, as part of the IMPAKT study (EudraCT number: 2016-004197-17, NCT: 03076151) sponsored by the University Hospital of Limoges and complying with the legal requirements of the Declaration of Helsinki, Good Clinical Practice and the International Conference on Harmonization guidelines. The protocol received approval from an Independent Ethics Committee (12/08/2016) and authorization from the French National Agency for Medicines and Health Products Safety (04/26/2017). Human blood was procured in line with WHO Guiding Principles on Human Cell, Tissue and Organ Transplantation and patients did not oppose to further utilization of their samples and data for research purposes. For the present study, we analyzed blood samples collected in EDTA, BD Vacutainer at 0, 20 and 40 min, 1, 2, 3, 4, 6 and 9 h after tacrolimus intake, 3 months after transplantation, from 5 fast metabolizers (homozygous or heterozygous for CYP3A5*1) and 7 slow metabolizers (homozygous for CYP3A5*3). We also analyzed samples collected at T_{max} (based on the individual concentration-time curves) on

days 7 and 30 post-transplantation from the same patients.

Peripheral Blood Mononuclear Cells (PBMC) were isolated using a Ficoll-gradient (see [Supplementary material and methods](#)) from leftovers of whole blood collected at T0 from transplant patients previously identified as fast or slow metabolizers. These samples had previously been accrued to the Limoges University Hospital biobank CRBioLim, authorized by the French ministry of health (No. AC-2016-2758). In accordance with the European general data protection regulation (GDPR 2016/679), patients were informed and this retrospective study was registered by the data protection officer (DPO) of Limoges University Hospital.

After defecation of PBMC and whole blood samples with a mixture of methanol and a saturated zinc sulfate solution (70/30, by volume), supernatants were submitted to solid-phase extraction on Oasis® HLB cartridges. The concentrations of tacrolimus and its metabolites were measured in patient blood using LC-HRMS with the TripleTOF® 5600+ instrument (Sciex, France) and, due to very low concentrations, in PBMC using HPLC-MS/MS in the MRM mode on an 8060 triple quadrupole mass spectrometer (Shimadzu, France).

2.3. Pharmacodynamics of M-I and pharmacodynamic competition with tacrolimus

2.3.1. In silico experiments

We modeled the [ligand-FKBP12] and [ligand-FKBP12-calcineurin A (CNA A) & calcineurin B (CNA B) complexes with all identified forms of tacrolimus and metabolites. Tacrolimus and metabolites were modeled using the Avogadro software [17] and the tacrolimus structure available in the Protein Data Bank (<https://www.rcsb.org/>, PDB) under the code 1FKJ as the original template (<https://www.rcsb.org/structure/1FKJ>) [18]. Relative internal stabilities were assessed at the density functional theory (DFT) M06-2X/6-31+G(d,p) level in the vacuum (see [Supplementary Table 1](#)) [19]. The FKBP12 structure was modeled based on the X-ray crystallography resolved structure under the code: 1FKJ. [Ligand-FKBP12] complexes were built by superimposing pipicolate moieties onto co-crystallized tacrolimus coordinates. Calcineurins A (b-Isoform) and B were modeled based on structures resolved by X-ray crystallography and available in the PDB using the code 4OR9, (<https://www.rcsb.org/structure/4OR9>). However, the C-terminal domain (residues 388–524) containing the autoinhibitory segment and the autoinhibitory domain [20] was not modeled, assuming an active conformation. [Ligand-FKBP12-CNA-CNB] complexes were built using the crystallized bovine structure available in the PDB under the code 1TCO as the structural template [21] (<https://www.rcsb.org/structure/1TCO>). They also included four Ca⁺⁺ ions bound to CNB.

Molecular dynamics (MD) simulations were conducted in three replicas and in 100 ns and 1 μs respectively for [ligand-FKBP12] and [ligand-FKBP12-CNA-CNB] complexes in water using 0.15 M KCl concentration. Data are shown as means ± standard deviations (STD). Structural analyses (Root-mean-squared deviation - RMSD, H-bond counting, coulombic and vdW interaction energies) were performed using the last 400 ns (100 ns) of MD trajectories for CN-FKBP12-Ligand (FKBP12-ligand). Binding affinities of tacrolimus and its metabolites for FKBP12 were evaluated by means of absolute binding free energy calculations using alchemical transformation. Statistical analyses of alchemical binding free energies were done using six independent replicas from six different starting geometries.

2.3.2. In vitro and ex-vivo experiments

2.3.2.1. FKBP12 binding by tacrolimus and its metabolites. Binding affinity was determined by Spectral Shift using the Monolith X instrument (Nano Temper Technologies, Cambridge, MA, USA) following the manufacturer's protocol. Briefly, 100 nM of recombinant human His-Tag FKBP12 protein (Abcam, ab85840) were labeled using 50 nM of

RED-tris NTA 2nd generation dye (NanoTemper Technologies, Cambridge, MA, USA), which labels the N-Terminus His Tag group. The labeled FKBP12 protein at 50 nM was mixed with serially diluted concentrations of either tacrolimus or its M-I metabolite in a 0.15–5 μM concentration range in PBS containing 0.05 % Tween 20 and 2.5 % DMSO. Sixteen premium capillaries were loaded, and measurements were carried out at 25 °C using medium IR laser power and 80 % LED excitation. Data of three independent measurements were analyzed (MO.Affinity Analysis software version 2.5.4, NanoTemper Technologies) using the 670 nm/650 nm signal ratio. Kd modeling was applied on curves with a vertical offset correction to determine the Kd constant.

2.3.2.2. NFAT nuclear translocation. The Jurkat-Lucia NFAT cell line (InvivoGen, San Diego, CA, USA), stably transfected with an NFAT luciferase reporter vector, was used to assess NFAT nuclear translocation in the presence or absence of tacrolimus and its metabolites. After 48 h of proliferation, 3.6×10^5 Jurkat-Lucia NFAT cells were exposed for 18–24 h to different conditions: negative control, 1 % ethanol; positive control, PMA 50 ng/mL, ionomycin 3 μg/mL, and 1 % ethanol; conditions tested: stimulation with 50 ng/mL PMA and 3 μg/mL ionomycin, concomitant to the addition of tacrolimus, purified M-I and metabolite pool in 1 % ethanol (each at 1, 10, 100, 1000 pg/mL, alone or in combination at equivalent concentrations). The luciferase assay was then performed following the manufacturer's instructions and luminescence reading using a Victor Nivo multimode microplate reader (Perkin Elmer, France).

2.3.2.3. IL-2 secretion measurement by ELISA. Jurkat E6.1 Clone cells were stimulated with PMA/Ionomycin (50 ng/mL and 1 μg/mL final concentrations) for 16 h at 37 °C. Concomitant to stimulation, cells were treated with tacrolimus, purified M-I, metabolite pool, alone or in combinations at equivalent concentrations in 1 % ethanol (10, 100, 1000 pg/mL). After incubation for 16 h, supernatants were collected and analyzed for human interleukin-2 (hIL-2) by ELISA (ELISA MAX™ Deluxe Set Human IL-2, BioLegend, San Diego, CA, USA) following the manufacturer's protocol and using a Victor Nivo multimode microplate reader (Perkin-Elmer, France).

2.3.2.4. One-way mixed lymphocyte reaction (MLR). PBMC from pairs of ABO-matched blood donors were used as responder and stimulator, respectively. The day before the experiments, frozen PBMC aliquots were thawed in RPMI 1640, GlutaMAX™, HEPES supplemented with 10 % FBS and 100 UI/mL Penicillin/Streptomycin and incubated at 37 °C in humidified 5 % CO₂. Stimulator cells were pre-treated with mitomycin C (50 μg/mL) for 45 min at 37 °C and used after extensive washing. 2×10^5 responder PBMC were then co-cultured with 1×10^5 stimulator PBMC in flat-bottomed 96-well plates. Stimulator cells from autologous PBMC were used as negative controls. The plate wells were spiked with the treatment preparations to be tested (ethanol 1 %, tacrolimus, metabolite pool, purified M-I alone or combined at 0.5 ng/mL or 1 ng/mL), completed with culture medium to reach a final volume of 200 μl per well and incubated for 5 days. Proliferation was assessed using the CellTiter 96® Aqueous Cell Proliferation Assay and absorbance reading was done using an Enspire® multimode reader (Perkin-Elmer, France).

2.4. Statistical analyses

Quantitative data are expressed as means ± standard error of the mean, and, unless otherwise indicated, all the results presented correspond to at least three independent repeats. Group comparisons were made using the Student's t-test, or one way ANOVA followed by the Dunnett multiple comparison test, with GraphPad Prism 10.

3. Results

3.1. Metabolic profiles of tacrolimus after incubation with HLM

Micro-LC-HRMS analysis of tacrolimus and its metabolites first focused on the detection of demethylated products. Tacrolimus in the incubation medium without microsomes (blank 2) was monitored

through its sodium adduct at $m/z = 826.4$, revealing three peaks with close retention times ($t = 20.0, 20.4$ and 20.9 min) (Supplementary Fig. 1) and similar fragmentation patterns. Interestingly, after incubation of tacrolimus with human liver microsomes (HLM), a fourth peak with the same m/z was observed at $t = 16.5$ min, with the same fragments as tacrolimus as well as other, specific fragments. This suggests that this fourth peak is a more hydrophilic isomer of tacrolimus.

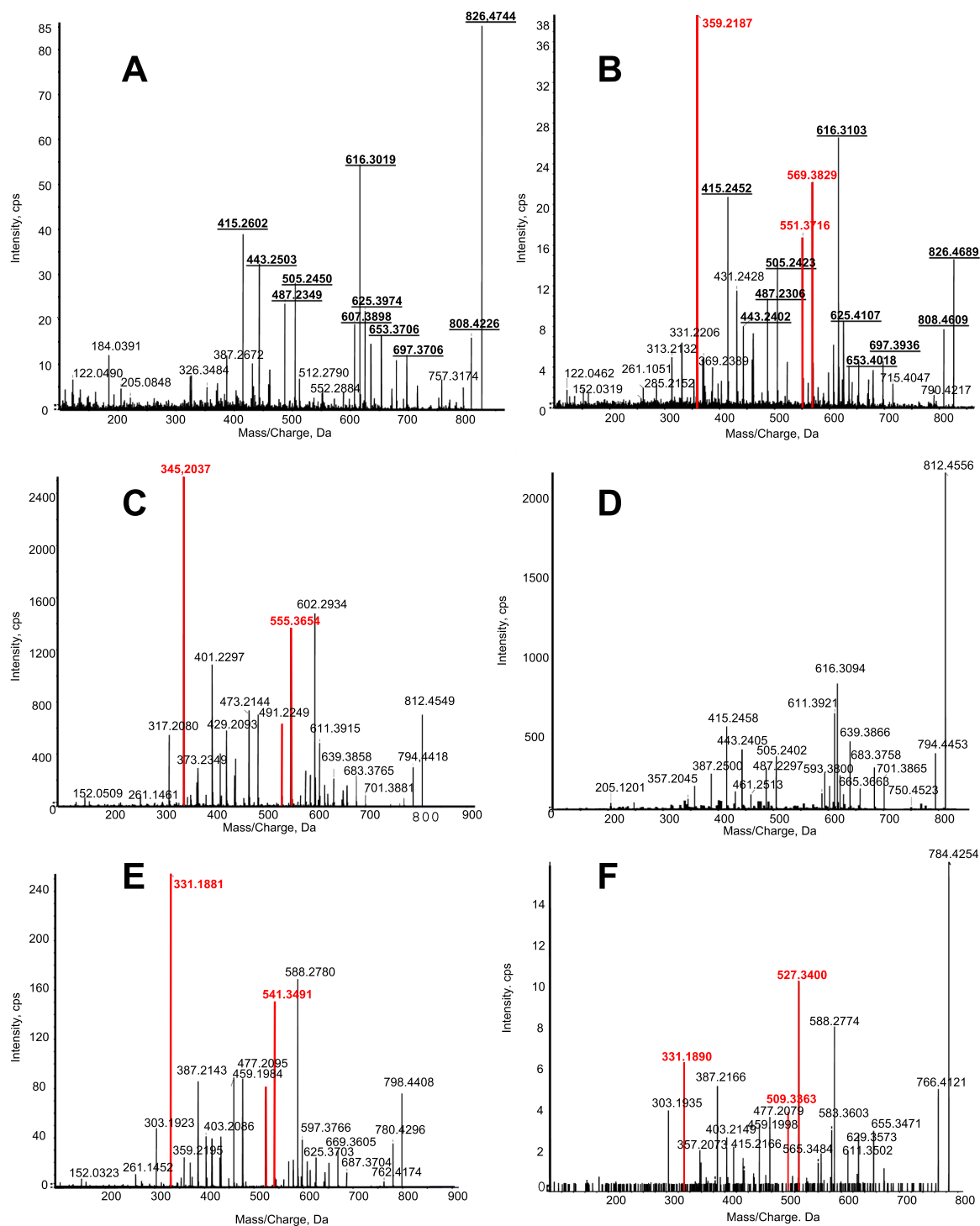


Fig. 1. High-resolution enhanced product ion spectra acquired, after incubation of tacrolimus with Human Liver Microsomes, at: (A) 21.05 min for tacrolimus (precursor ion, m/z 826.5); (B) 16.02 min for open-ring tacrolimus (precursor ion, m/z 826.5); (C) 17.60 min for M-I, one of the mono-demethyl-tacrolimus metabolites (precursor ion, m/z 812.5); (D) 20.30 min for M-II, another mono-demethyl-tacrolimus metabolite (precursor ion, m/z 812.5); (E) 15.49 min for a di-demethyl-tacrolimus metabolite (precursor ion, m/z 798.5); and (F) 14.82 min for tri-demethyl-tacrolimus (precursor ion, m/z 784.5). The most abundant fragments specific of the open-ring structure and their respective m/z are in red.

Using the same analytical conditions, different metabolites were observed with m/z ratios corresponding to mono-, di- and tri-demethylated tacrolimus sodium adducts, respectively at $m/z = 812.4$, 798.4 and 784.4 . Particular attention was paid to mono-demethylated metabolites (dT) since they were the most abundant (Fig. 1). According to the literature, demethylation can occur at C-13, C-31 and C-15 positions leading to M-I, M-II and M-III, respectively. Micro-LC-HRMS runs were thus searched for peaks exhibiting the parent ion ($m/z = 812.4$) and fragments specific for M-I/M-III ($m/z = 602.3$, since demethylation on C-13 and C-15 is undistinguishable) or M-II ($m/z = 616.3$) as reported by Dai et al. [22]. Six peaks were observed with the $826.4 \rightarrow 602.3$ transition. M-I and M-III were assigned based on retention times and intensity following previous reports [5], M-I being the earliest and most abundant, and M-III the second most abundant. The other peaks with the fragment $m/z = 602.3$ were regarded as M-I and/or M-III isoforms (as already proposed for M-I [23]). Two peaks were observed at the $826.4 \rightarrow 616.3$ transition, only at high tacrolimus and microsomes concentrations, and were considered as two M-II isomers (Fig. 1A). Finally, four and two peaks were observed for di- and tri-demethylated tacrolimus sodium adducts, respectively.

3.2. Structural elucidation of tacrolimus metabolites

Enhanced Product Ion (EPI) spectra were investigated to decipher the structure of tacrolimus and its metabolites (Fig. 1, and Supplementary Figs. 1–3), with help from the literature. Surprisingly, the EPI spectrum of the tacrolimus peak with the shortest retention time (the new isomer, Supplementary Fig. 1) showed a fragmentation pattern different from that of the other tacrolimus isoforms: seven additional fragments were observed, with the most abundant at $m/z = 569.3829$, 551.3716 and 359.2193 (Fig. 1). Four mono-demethylated metabolites out of six showed the same pattern, negatively shifted by m/z 12. Three distinct fragmentation pathways were thus hypothesized based on the fragments observed for tacrolimus, its new isomer and its metabolites (Fig. 2). Pathway 1 is initiated by a loss of C_6H_9NO and pathway 2 by a loss of $C_{13}H_{22}O_2/C_{12}H_{20}O_2$. Pathway 3, observed for the new tacrolimus isomer, M-I, M-III, and two isomers thereof, is characterized by a supplemental loss of $C_{11}H_{15}NO_6$ (Fig. 2 B), confirming a backbone structure different from that of tacrolimus. *In silico* fragmentation analyses as well as the fragmentation pattern proposed by Dai et al. [22] led us to hypothesize that the fragmentation pathway 3 corresponds to a structural rearrangement of the tetrahydropyranyl ring, with ring opening and apparition of a geminal diol moiety on C-10 (so-called open-ring structure) (Fig. 2). Since the EPI spectrum of M-II does not exhibit pathway 3 fragments, M-II is not expected to adopt this open-ring structure.

M-I, the mono-demethylated metabolite with the shortest retention time and highest intensity, was purified at > 90 % and characterized by NMR (Supplementary Fig. 2; Supplementary Table 2). NMR assignment was very similar to that already published for 13-O-desmethyl-tacrolimus [24] in $CDCl_3$ at 300 K, with a major *trans*-isomer 1a under the main chromatographic peak and a minor *cis*-isomer 1b under a shoulder in the peak descent (as also previously reported and observed here for commercial tacrolimus). The 1H and ^{13}C chemical shifts for the major and minor isomers were similar, with chemical shift differences that did not exceed the NMR experimental error, *i.e.* 0.1 ppm for ^{13}C and 0.01 ppm for 1H , respectively. In addition, the 73:27 proportion of the *trans* 1a and *cis* 1b isomers was identical to that of the previous publication, confirming that the metabolite considered as M-I is actually 13-O-desmethyl-tacrolimus [24]. Schüler et al. [24] observed from HMBC experiments a significant correlation between H-C-13 and C-10 in isomer 1a. This may be interpreted as the formation of a furan ring, obtained by the opening of the hemiketal in which H-C-13 and C-10 are separated by only three bonds in *trans*-isomer 1a and *cis*-isomer 1b. Unfortunately, due to significantly lower amounts of the pure compound available compared to the previous study, we could not observe this, nor the H-C-14/C-10, correlations using HMBC experiment. However,

according to the NMR similarity and the previously reported metabolite structure, *trans/cis* isomers of 13-O-desmethyl-tacrolimus with a furan structure (Fig. 2C) were assumed, at odds with the high-resolution mass spectrometry results.

3.3. Kinetics of tacrolimus metabolism

The normalized kinetic profiles of tacrolimus exhibited a decrease over time, while the abundance of the open-ring tacrolimus structure increased over the first 20 min and then slowly decreased. Open-ring tacrolimus is thus expected to be a metabolization intermediate or final product. Likewise, the kinetic profiles of mono-demethylated tacrolimus exhibited a maximum concentration at $t = 20$ min and then decreased over time (Supplementary Fig. 3). The kinetic profiles of M-I and open-ring tacrolimus did not exhibit significant differences.

3.4. Tacrolimus metabolites and metabolic ratios in patient blood and PBMC

The presence and structure of tacrolimus metabolites were investigated in blood samples obtained from patients on tacrolimus, using High Resolution Mass Spectrometry in the Multiple Reaction Monitoring (MRM-HR) mode to obtain both high sensitivity and high specificity. M-I, M-III and at least one isomer were consistently observed in all blood samples, whereas M-II was never detected. The retention times and EPI spectra of M-I and M-III in patient blood were the same as those observed in *in vitro* experiments (Fig. 3A&B), which means that they also had an open-ring structure. In contrast, open-ring tacrolimus was not observed.

Additionally, blood samples were collected from patients who carried at least one active CYP3A5*1 allele ($n = 5$) and from others devoid of this allele ($n = 7$). At T_{max} , tacrolimus blood concentrations were similar between the two groups on day 7, months 1 and 3 post-transplantation (Fig. 3C). In contrast, the M-I/TAC C_{max} ratio showed notable differences: CYP3A5*1 allele carriers exhibited a significantly higher ratio to M-I on day 30 ($p = 0.0008$) and even more so on day 90 ($p = 0.012$) post-transplantation than non-carriers, despite similar tacrolimus blood concentrations. CYP3A5 expressers exhibited lower M-III/TAC C_{max} ratios than non-expressers on day 7 ($p = 0.0036$), but not on days 30 and 90. The blood kinetic profile of the metabolites was studied using all samples collected over 9 h post-dose on day 90 post-transplantation in the same patients, to calculate the area under the concentration vs. time curve (AUC_{0-9h}). It confirmed the absence of significant differences in tacrolimus AUC or M-III/TAC AUC ratio depending on the CYP3A5 genotype, whereas the M-I/tacrolimus and M-I isoform/TAC AUC ratios were significantly higher in CYP3A5*1 allele carriers ($p = 0.0061$ and $p = 0.0013$, respectively) (Fig. 3D). Immune cells being the therapeutic target of tacrolimus, we also compared tacrolimus trough concentrations (C_0) and M-I/TAC C_0 ratios in PBMC from poor and extensive metabolizers on tacrolimus. Consistent with regular dose adjustment compensating for patient CYP3A5 genotype, tacrolimus pre-dose concentrations in PBMC (Fig. 3E) and blood (Fig. 3F) were not statistically different between patient groups, whereas M-I/TAC C_0 ratios were significantly higher in PBMC from extensive metabolizers than from poor metabolizers ($p = 0.1440$, 0.0812 , and 0.0039 , respectively).

3.5. MD simulations of FKBP12 binding by tacrolimus and metabolites

For the sake of readability, tacrolimus and its metabolites were coded depending on their macrolide ring structure, *i.e.* n, o and f for the “normal”, open-tetrahydropyranyl and tetrahydrofuran ring structures, respectively. TACn, TACo, M-In, M-Io, M-If, M-IIn, M-IIIn and M-IIo were all considered, whereas M-II was only considered (and observed) in the closed-ring form (M-IIn). Internal energies of the M-I optimized structure in vacuum obtained at the DFT level (Supplementary Table 1) suggested that M-If is as stable as M-Io, and

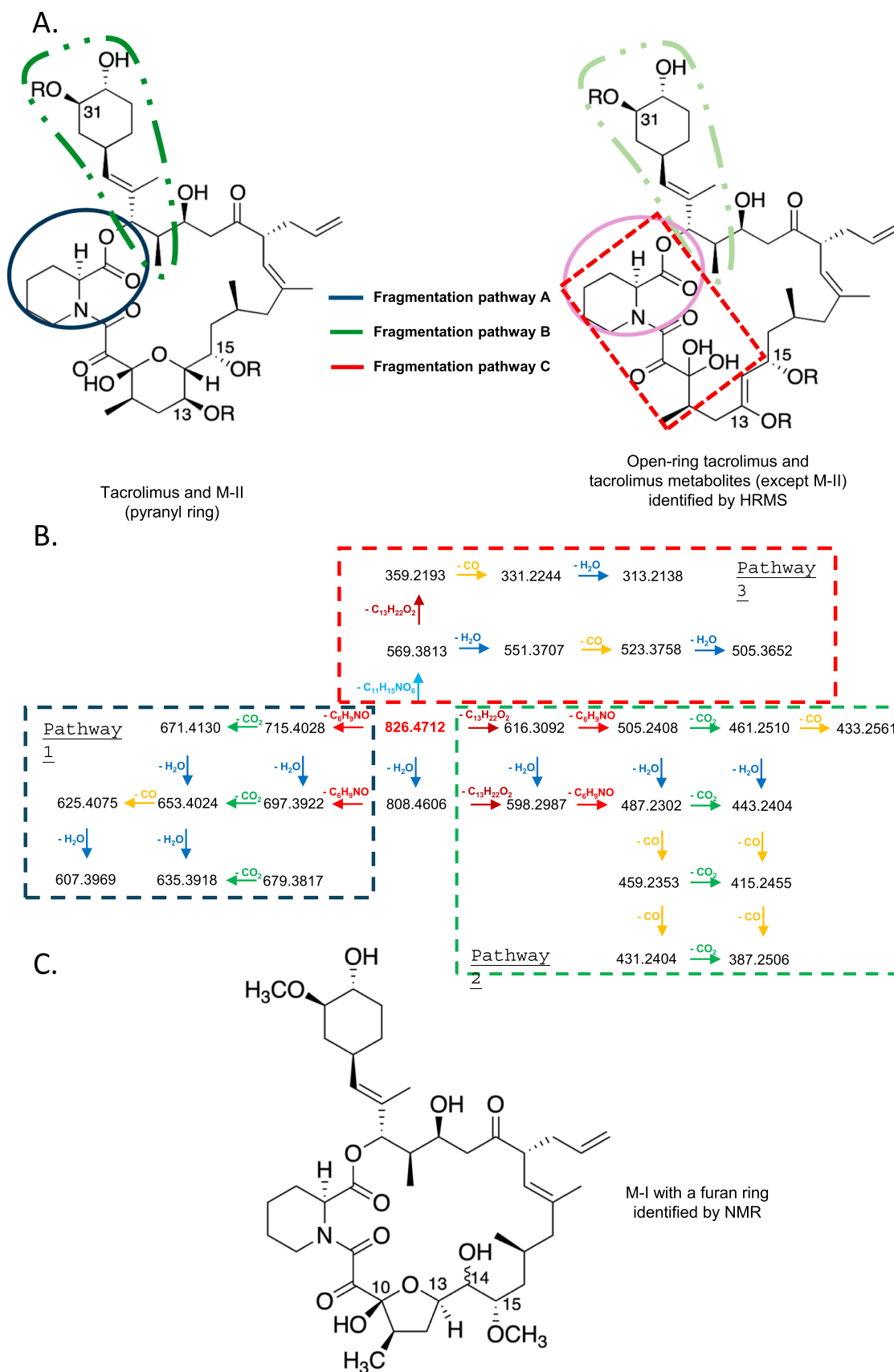


Fig. 2. Proposed chemical structures (A) and high resolution mass spectrometry fragmentation pathways and fragmentation intermediates (B) of pyranyl-ring and open-ring tacrolimus. M-I furan-ring structure identified by NMR (C).

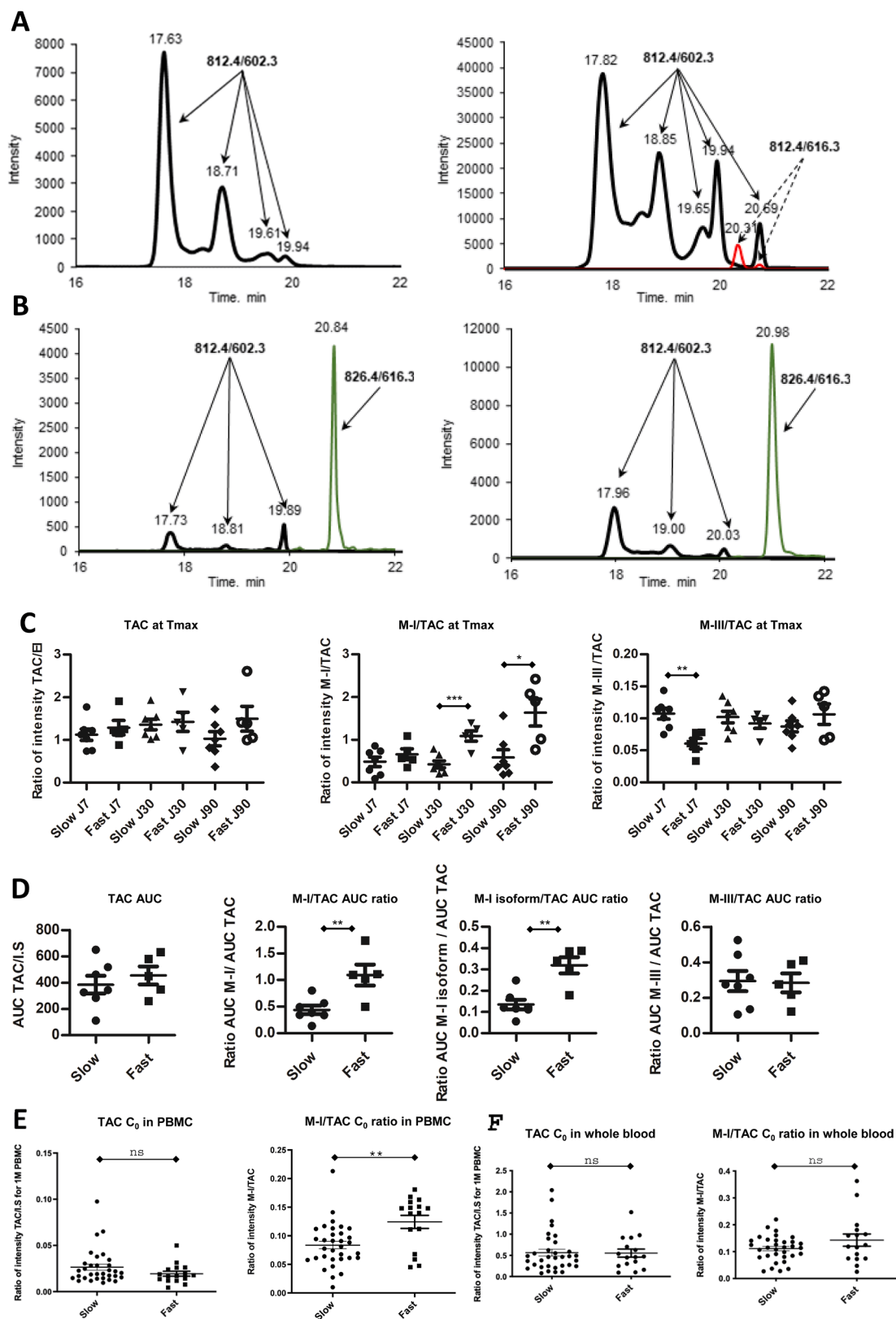


Fig. 3. Determination of tacrolimus metabolites in transplant patients' blood and PBMC and comparison with *in vitro* findings. (A) Unit mass chromatograms of tacrolimus demethylated metabolites (M-I, M-III and their respective isomers in black, M-II and its isomer in red) detected in the incubation media after metabolization with human liver microsomes at 0.5 mg/mL (left) and 5 mg/mL (right). (B) Representative chromatograms of tacrolimus metabolites in patients' whole blood, with tacrolimus desmethyl-metabolites in black and tacrolimus in green. Left: from a slow metabolizer, right: from a fast metabolizer. (C) Tacrolimus concentration and M-I/tacrolimus and M-III/tacrolimus concentration ratios at Tmax in transplant patients' blood at 7-, 30- and 90-days post-transplantation. (D) Tacrolimus AUC and metabolites/tacrolimus AUC ratios in whole blood from transplant patients at 90 days post-transplantation. (E–F) Pre-dose (C0) tacrolimus concentrations and M-I/tacrolimus ratio in transplant patients at least 30 days post-transplantation, (E) in PBMC and (F) in whole blood.

that both are $\sim 5 \text{ kcal.mol}^{-1}$ more stable than M-In. In contrast, TACn and M-III_n exhibited lower energies than their open forms (*i.e.* TACo and M-IIIo).

No significant structural difference with the X-ray structure [18] was observed, regardless of the ligands and their macrolide structure, as pictured by time-dependent RMSD over MD simulations. For instance, RMSD calculated for the average structure from [TACn-FKBP12] simulations (Supplementary Fig. 4) ranged from 0.58 ± 0.08 to $0.68 \pm 0.09 \text{ \AA}$, showing global conservation of the [ligand-FKBP12] complex regardless of the ligand structure (Fig. 4A). In other words, demethylation, tetrapyranyl ring opening (TACo, M-Io and M-IIIo) or rearrangement (M-If) are unlikely to modify FKBP12 binding with respect to the closed-ring structures (TACn, M-In, M-II_n and M-III_n). These results are consistent with the calculated non-covalent interaction energies

between the ligands and FKBP12, which exhibit similar values for all systems (Fig. 4B). This can be explained by H-bond analyses stressing the key role of ³⁸Asp, ⁵⁵Glu, ⁵⁷Ile and ⁸²Tyr for FKBP12 binding to the pipecolate moiety conserved by all metabolites (Fig. 4A&B). The H-bond network is maintained by an average of 3.00 ± 0.07 H-bonds between ligands and these amino acid residues, among which ⁸²Tyr, ³⁸Asp, ⁵⁵Glu and ⁵⁷Ile contribute for *ca.* 30.2, 28.8, 24.5 and 16.5 %, respectively. These results are also consistent with previous studies [25, 26] showing that the pipecolate moiety is mandatory for tacrolimus binding, while the demethylation sites (*i.e.*, C-13, C-31 and C-15) are distant from the key interacting FKBP12 residues.

Binding free energies were then calculated to assess differential binding affinity between tacrolimus and its metabolites. The robustness of this approach was first confirmed by a very low free energy difference,

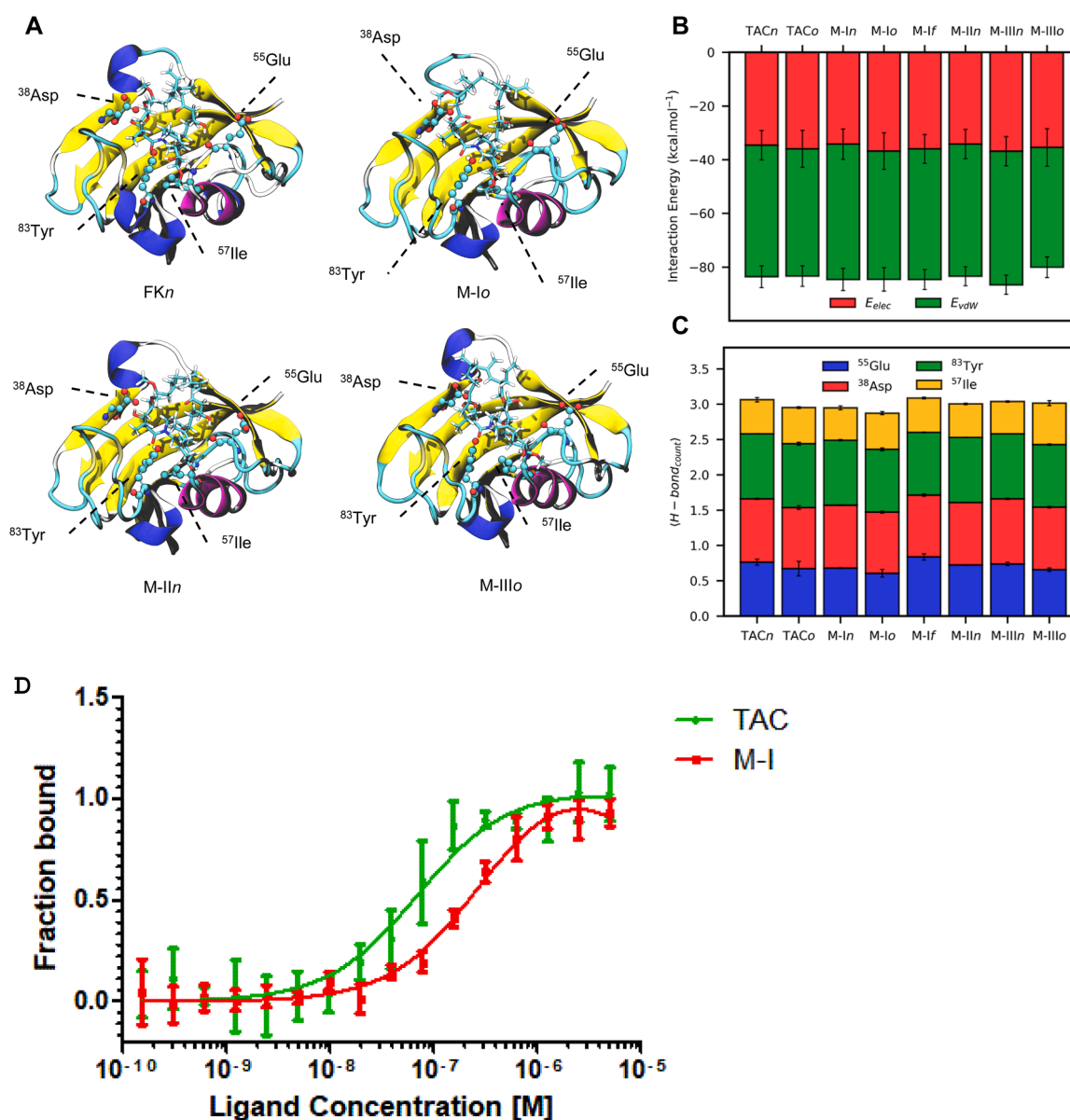


Fig. 4. (A) Representative structures of FKBP12 bound to tacrolimus (TACn, upper left), open-ring M-I (M-Io, upper right), M-II (lower left) and open-ring M-III (M-IIIo, lower right). Ligands and key FKBP12 binding residues are respectively depicted using ‘Balls and sticks’ and ‘Licorice’ representations. (B) Calculated Lennard-Jones (green) and Coulombic (red) non-covalent interaction energies (kcal.mol^{-1}) between FKBP12 and tacrolimus or metabolites. Standard deviations were calculated separately for Lennard-Jones and Coulombic terms over $3 \times 110 \text{ ns}$ MD simulations from three replicas. (C) Average H-bond count between FKBP12 key binding residues and tacrolimus and its metabolites. Standard deviations were separately calculated for each H-bond partner over $3 \times 110 \text{ ns}$ MD simulations from three replicas. (D) Normalized spectral shift dose-response curves of tacrolimus (green circles) or M-I (red squares) with 50 nM His tagged FKBP12. Error bars represent standard error of $n = 3$ values.

lower than the chemical accuracy for alchemical methods (*i.e.*, $\sim 2.0 \text{ kcal.mol}^{-1}$) [27], between theoretical and experimental results for the TACn-FKBP12 bound system [28], as well as with former theoretical studies [25]. In line with structural and H-bond analyses, no significant difference in terms of binding free energy (Table 1) was observed among all the ligands for FKBP12 binding.

3.6. MD simulations of CN-FKBP-ligand complex dynamics depending on tacrolimus and metabolites structure

MD simulations of [ligand-FKBP12-CNA-CNB] complexes were performed to provide structural hints on FKBP12-ligand binding to CNs. The complexes included CNA, CNB and FKBP12 (based on X-ray structures [21,29]), bound to tacrolimus or its metabolites. FKBP12 remained bound to CNs along simulations regardless of the ligand, but RMSD analysis revealed that the structural dynamics of FKBP12-ligand with CNs differed depending on the tacrolimus and metabolite structures. MD simulations revealed a rocking motion of FKBP12 and the CNA lobe motion around CNB Binding Helix (BBH), similar to the single residue variant FKBP12-CNs systems in fungi [29].

To picture the overall difference between ligands, FKBP12 supra-molecular variabilities were assessed using two structural parameters, namely the angle between CAN BBH and FKBP12 (θ) and the twist angle between CAN catalytic lobe and FKBP12 (φ , see Fig. 5B). While closed ring ligands (*i.e.*, TACn, M-In, M-If, M-IIIn and M-IIIn) tended to maintain FKBP12 stable over simulations, those with an open-ring structure (*i.e.*, TACo, M-Io, M-IIIo) significantly deviated and exhibited wider distribution onto the $\varphi \times \theta$ conformational space (Fig. 5).

Such observations are consistent with different H-bond networks between FKBP12-ligand and CNA&B (Fig. 5C and 5D). For instance, simulations with TACn stressed that $^{353}\text{Asn}_{\text{CNA}}\text{-}^{90}\text{Glu}_{\text{FKBP12}}$, $^{368}\text{Lys}_{\text{CNA}}\text{-}^{55}\text{Glu}_{\text{FKBP12}}$, $^{122}\text{Asn}_{\text{CNB}}\text{-}^{43}\text{Arg}_{\text{FKBP12}}$ and $^{127}\text{Gln}_{\text{CNB}}\text{-}^{48}\text{Lys}_{\text{FKBP12}}$ H-bonds maintained interactions between FKBP12 and CNA&B. The H-bond networks between CNA on the one hand, and FKBP12 bound to the open-ring (TACo, M-Io and M-IIIo) or tetrahydrofuranlyl (M-If) structures on the other hand, were smaller than those with the corresponding tetrahydropyranlyl (TACn, M-In, M-IIIn) ring. Interestingly, M-If was the only structure increasing H-bonds between FKBP12 and CNB. This was confirmed by the global non-covalent interaction energies between ligand-bound FKBP12 and CNs (Fig. 5E and Supplementary Fig. 4). All M-I isomers and M-IIIo led to significantly less favorable binding interactions between FKBP12 and CNA than tacrolimus (Supplementary Fig. 4). However, the stronger interactions between M-If-bound FKBP12 and CNB led to significantly stronger interaction energy between FKBP12 and CNB, which compensated its weaker binding with CNA (Fig. 5). Interestingly, FKBP12 ^{88}His was previously described as crucial for CN binding [29]. The distance between the cyclohexanyl moiety of tacrolimus or its metabolites and $^{88}\text{His}_{\text{FKBP12}}$ was measured, showing that ring opening was associated with a broader ligand- ^{88}His distance distribution than close-ring ligands. Less contact between ligands and ^{88}His in turn led to a higher flexibility of the 80 s loop (Supplementary

Table 1

[FKBP12-ligand] Binding free energies calculated at 293 K and 310 K obtained by means of softcore alchemical calculations.

Molecules		20°C		37°C
		ΔG_{theo}	ΔG_{exp}	ΔG_{theo}
Closed form	TACn	-11.1 ± 1.2	-12.2 ± 0.1^a	-7.8 ± 2.0
	M-In	-11.2 ± 2.2	-	-8.3 ± 2.0
	M-IIIn	-11.4 ± 2.1	-	-8.2 ± 1.9
	M-IIIn	-11.8 ± 2.2	-	-8.5 ± 1.9
	TACo	-10.4 ± 2.4	-	-7.2 ± 2.4
Open form	M-Io	-11.1 ± 2.4	-	-8.0 ± 2.1
	M-IIIo	-11.6 ± 2.1	-	-8.5 ± 1.9
	M-If	-11.4 ± 2.5	-	-8.1 ± 2.4

^a From Refs. [26,28].

Fig. 5). Such flexibility may be associated with a lower CN inhibition potency [29].

3.7. Pharmacodynamic interactions between tacrolimus and its metabolites in vitro

The Kd of tacrolimus and M-I metabolite with FKBP12 at 25°C, determined by fitting the binding curves obtained from the mean spectral shift signal, were 35.7 nM (CI95 %: 20–63.6 nM) and 184 nM (CI95 %: 139–245 nM confidence interval), respectively (Fig. 4D).

We used Jurkat-Lucia NFAT cells, which contain an NFAT-inducible luciferase reporter, to measure NFAT translocation (Fig. 6A) and Jurkat E6.1 cells to measure IL2 secretion using an ELISA assay (Fig. 6B). Cell stimulation with phorbol myristate acetate (PMA) and ionomycin (positive control), known activators of the calcineurin pathway, consistently increased luciferase activity and IL2 production above those of the respective negative control, thus indicating higher NFAT translocation to the nucleus and activation of T lymphocytes, respectively. Concomitant treatment of cells with 1–2000 pg/mL tacrolimus decreased both NFAT translocation and IL2 secretion in a dose-dependent manner. Interestingly, cells incubated with purified M-I alone and the metabolite pool both failed to significantly decrease luciferase activity (Fig. 6A) or IL2 production (Fig. 6B), except for M-I at the highest concentration (1 ng/mL). Moreover, activated cells exposed to a mixture of 1–1000 pg/mL tacrolimus and either 1–1000 pg/mL of purified M-I or the metabolite pool had only slightly lower luciferase activity and IL2 secretion than when exposed to tacrolimus alone. Tacrolimus and M-I IC50 were derived from the dose-response curves of tacrolimus alone or in combination with M-I on IL2 secretion at 12 h by Jurkat E6.1 cells (Fig. 6C), yielding values of 32.07 pg/mL for tacrolimus and 99.95 pg/mL for M-I.

3.8. Pharmacodynamic interactions between tacrolimus and its metabolites ex vivo

We next evaluated IL2 secretion by healthy volunteers' PBMC stimulated with PMA and ionomycin (Fig. 6D) and confirmed that tacrolimus alone decreased IL2 secretion and that its co-incubation with M-I or the metabolite pool (ratio 1:1) did not significantly modify its inhibitory effect.

MLR experiments showed substantial PBMC proliferation in response to allogeneic stimulation by PBMC from another healthy volunteer, as opposed to minimal proliferation in response to autologous stimulation (Fig. 6E). PBMC proliferation was inhibited by tacrolimus at 0.5 ng/mL and 1 ng/mL. Adding either M-I or the metabolite pool to tacrolimus did not change tacrolimus-mediated immunosuppression, whatever the ratio between tacrolimus and its metabolites.

4. Discussion

This extensive study had the rather unusual aim of assessing possible pharmacodynamic interactions between a parent compound and its metabolites, at a time when companies are developing subcutaneous formulations of tacrolimus (*i.e.* bypassing the hepatic first pass), and as a pre-requisite to investigating further the toxicity of these metabolites. Specifically, tacrolimus, an important transplantation drug, acts through the formation of a pentamer with its intracellular binding protein FKBP12, calcineurin A, calcineurin B and calmodulin (and Ca^{2+}) that inhibits calcineurin NFAT dephosphorylation activity. Preliminary molecular modeling showing equivalent binding to FKBP12 of tacrolimus and its metabolites prompted us to investigate whether these metabolites, starting with M-I, the main one, may interfere with tacrolimus pharmacodynamics. Actually, the literature reports that only M-II, a very minor tacrolimus metabolite, retains some calcineurin inhibition activity [12]. However, such activity has been tested *in vitro* for each metabolite independently, and not in the presence of tacrolimus,

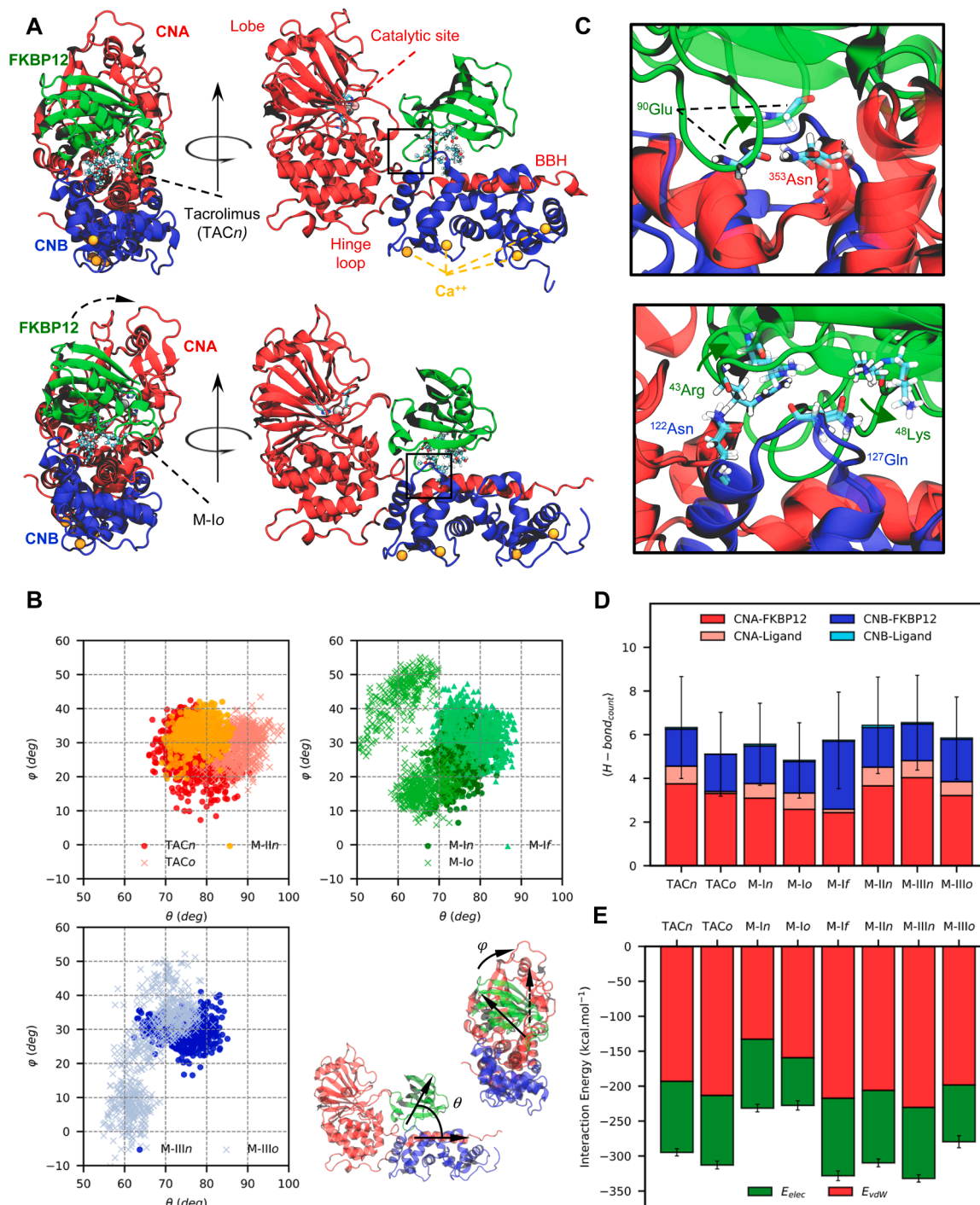


Fig. 5. (A) Representative structures of CN-FKBP12 bound to tacrolimus (TACn, top) and open-ring M-I (M-Io, bottom) with front- (left) and side-views (right). CNA, CNB and FKBP12 are depicted in red, blue and green, respectively. Fe-, Zn- and Ca-atoms are represented using VDW spheres. Ligands are shown using 'Balls and Sticks' representations. (B) 3D-distributions of θ and φ angles for tacrolimus TACn and M-IIn-bound systems (upper left), M-I-bound systems (i.e. M-IIn, M-Io and M-IIf, upper right) and M-III-bound systems (i.e. M-IIIIn and M-IIIo, lower left). Normal, open and tetrahydrofuranyl (only for M-I) structures were plotted using spheres and crosses, respectively. θ and φ angles were defined to represent the rocking motion and closing angle between the CNA CNB Binding Helix domain and FKBP12 (lower right), respectively. (C) Superimposition of [TACn-FKBP12-CAN-CNB] and [M-Io-FKBP12-CAN-CNB] systems focusing on key H-bond displacement at CNA- (top) and CNB-FKBP12 (bottom) interfaces, the M-Io-bound system being made transparent. (D) Average H-bond counts between ligand-FKBP12 and CN partners, in which contributions from CNA-FKBP12 (red), CNA-Ligand (pink), CNB-FKBP12 (blue) and CNB-Ligand (cyan) pairs are reported. Standard deviations were calculated using the last 400 ns MD simulations from three replica per system. (E) Calculated Lennard-Jones (green) and Coulombic (red) non-covalent interaction energies (kcal.mol⁻¹) between FKBP12-Ligand pair and CNs pair. Standard deviations were calculated separately for Lennard-Jones and Coulombic terms over the last 400 ns MD simulations from three replica per system.

meaning that pharmacodynamic interactions have not been tested (which is not unusual since this is not a regulatory requirement).

We generated tacrolimus metabolites *in vitro*, characterized them by LC-HRMS, and then purified M-I and characterized it by LC-HRMS and NMR, with diverging results. HRMS identified an open-ring structure for an isoform of tacrolimus, M-I, M-III and 2 other mono-demethylated metabolites, whereas NMR identified M-I as a furanyl derivative with two isomers, corresponding to the rearrangement of the tetrahydropyranyl into a furan ring. This difference may be due to the conditions used with the two techniques. We verified that temperature had no influence. The different polarity of the solvents used may be an explanation. When assessing their octanol/water partition function (logP), M-If appears to be more lipophilic than M-Io, suggesting that the former may exhibit at higher abundance in apolar solvents, such as CDCl₃ used here for the NMR experiments, whereas M-Io may be favored in more polar solvents, such as water and acetonitrile used in MS. The formation of sodium adducts in the mass spectrometer electrospray source and high vacuum is even more likely to explain ring opening. Actually, theoretical chemistry estimates that rearrangement as either a furanyl ring or ring opening has exactly the same probability of happening as a result of CYP3A metabolism, and that both are more stable than the tetrahydropyranyl ring. The historical characterization of M-I in 1993 also used NMR after *in vitro* production of metabolites by HLM, but preparative chromatography was based on isocratic separation on a glass column at ambient pressure, and sample collection simply driven by the molecular mass assessed by chemical ionization, single-stage mass spectrometry [24]. This may explain why the authors found five isomers of M-I and two conformers (Ia to If) using NMR, when we found only the two conformers Ia and Ib. In contrast, they were able to formally characterize the furanyl ring of M-I, while we could only assume our structure was similar to theirs, due to the limited amount of pure compound.

We confirmed the presence of open-ring M-I and M-III in patient blood and PBMC, but it was also by means of electrospray ionization that favors sodium adducts. Therefore, we cannot infer the form(s) under which M-I is present in target cells and more importantly, as part of the pentamer complex. M-II did not show the characteristic fragments of the open-ring structure, suggesting the tetrahydropyranyl ring it shares with tacrolimus resists to the sodium adduct and may also be important for calcineurin inhibition.

Molecular modeling estimated that all tacrolimus metabolites, whether open-ring, furanyl, or pyranil (such as M-II) have an affinity towards FKBP12 similar to that of tacrolimus, whereas *in vitro* M-I had a 5-fold higher K_d than tacrolimus. Such a difference can be explained by (i) the chemical inaccuracy of alchemical binding free energies, which can reach ~ 2 kcal.mol⁻¹ (i.e., one order of magnitude of K_d) [27] and (ii) binding affinity temperature dependence, since calculations mimicked temperatures of 20 °C (to compare with former studies [25, 28]) or 37 °C (to estimate binding affinity *in situ*) (Table 1) while *in vitro* experiments were conducted at ambient temperature, i.e. between 18 and 25 °C. Tamura et al. reported that M-I binding affinity was 9.6 % of that of tacrolimus [30], which is in the same order of magnitude as our experimental results.

In silico, the FKBP12-metabolite complexes have differential binding to CNA&B as compared with tacrolimus (stronger for M-If, weaker for open-ring metabolites, equivalent for all tetrahydropyranyl compounds), which might result in differential effects on NFAT dephosphorylation. However, this did not translate into negative modulation of tacrolimus CN inhibition *in vitro*, but rather into a (small) additive effect. A possible explanation is that the binding capacity of FKBP12 (or rather of the pentamer, since it has been described as a single-step process) was probably not saturated in our experiments, where we used pharmacologically plausible concentrations of tacrolimus and metabolites, hence no strong competition can be seen. On the contrary, we found a very weak, positive pharmacodynamic interaction of M-I with TAC, consistent with previous results [30] and not likely to modify tacrolimus

efficacy in transplant patients.

One-way *ex-vivo* MLR experiments in the same concentration ranges confirmed that neither purified M-I nor a pool of tacrolimus metabolites dampened tacrolimus immunosuppressive activity.

Whole blood and PBMC concentrations of TAC metabolites in kidney transplant recipients are very small in blood and even smaller in PBMC. However, the apparent M-I/TAC peak ratios presented and used for comparative purposes in Fig. 3 must be corrected by an average mass spectrometry response factor of 3.4 in favor of M-I, meaning that M-I is more concentrated than it looks.

The structure of tacrolimus metabolites was established more than thirty years ago [5,6], and we thought that new characterization methods might be susceptible to unveil new metabolites or unexpected structures, which is the case with these open-ring metabolites. Their binding to FKBP12 was studied using separation of the bound/free forms by dextran charcoal adsorption [30] and their pharmacodynamic activity through a complex ELISA pentamer formation assay entailing polyclonal anti-calcineurin A antibodies, several phases of blocking residual binding sites, 6 incubation periods and 12 washings.

One limitation of this study is that we did not explore the individual interactions of other Tac metabolites with the parent drug. In particular, M-III, the second most abundant metabolite in patient blood and PBMC here, was reported to have a 16 % higher affinity for FKBP12 than tacrolimus. However, a mixture of Tac metabolites generated using human liver microsomes, with a distribution of metabolites close to that found in patient blood and PBMC, was tested in parallel to M-I with all *in vitro* and *ex-vivo* activity experiments and showed no specific activity or pharmacodynamic interaction with tacrolimus.

5. Conclusion

In conclusion, a mixture of tacrolimus metabolites produced by human liver microsomes as well as purified M-I showed no significant effects on NFAT dephosphorylation, IL2 secretion and mixed lymphocyte reaction and did not interfere with tacrolimus inhibition of the same tests. Therefore, dosing tacrolimus parenterally, i.e. shunting its important first pass effect is not expected to modify the drug pharmacodynamics.

CRedit authorship contribution statement

Hassan Aouad: Writing – review & editing, Writing – original draft, Methodology, Investigation, Formal analysis, Data curation. **Mélanie Campana:** Writing – review & editing, Writing – original draft, Validation, Supervision, Resources, Project administration, Funding acquisition, Conceptualization. **Rudy Mevizou:** Writing – review & editing, Writing – original draft, Methodology, Investigation, Formal analysis, Data curation. **Florent Di Meo:** Writing – review & editing, Writing – original draft, Supervision, Methodology, Investigation, Funding acquisition, Data curation. **Adolfo Lopez-Noriega:** Writing – review & editing. **Rodolphe Alves de Sousa:** Writing – review & editing, Methodology, Investigation. **Nicolas Giraud:** Writing – review & editing, Writing – original draft, Methodology, Investigation. **Gildas Bertho:** Writing – review & editing, Writing – original draft, Methodology, Investigation. **Jean-Sébastien Bernard:** Writing – review & editing, Methodology, Investigation. **Emilie Pinault:** Writing – review & editing, Methodology, Investigation. **Hélène Arnion:** Writing – review & editing, Methodology, Investigation. **François-Ludovic Sauvage:** Writing – review & editing, Writing – original draft, Methodology, Investigation, Formal analysis, Data curation. **Pierre MARQUET:** Writing – review & editing, Writing – original draft, Validation, Supervision, Resources, Project administration, Funding acquisition, Conceptualization.

Funding sources

This work was supported by the French Government's "Plan de relance" (ANR-19-CE17-0008-01) and by grants from the French Research Agency (ANR-21-CE18-0030-01, DIGPHAT 22-PESN-0017) and from Inserm and Région Nouvelle Aquitaine (AAP-NA-ESR 2019 VICTOR and 2023 MUSYPHA).

Data statement

Data are available from the corresponding author on reasonable request.

Declaration of Competing Interest

The authors declare the following financial interests/personal relationships which may be considered as potential competing interests: Melanie Campana reports administrative support and equipment, drugs, or supplies were provided by MedinCell SA. Rudy Mevizou reports administrative support and equipment, drugs, or supplies were provided by MedinCell SA. Pierre Marquet reports a relationship with MedinCell SA that includes: consulting or advisory, equity or stocks, and funding grants. Melanie Campana reports a relationship with MedinCell SA that includes: employment and equity or stocks. Alfonso Lopez-Noriega reports a relationship with MedinCell SA that includes: employment and equity or stocks. Pierre Marquet reports a relationship with Sandoz France that includes: consulting or advisory and funding grants. Pierre Marquet reports a relationship with Chiesi SA France that includes: consulting or advisory and funding grants. If there are other authors, they declare that they have no known competing financial interests or personal relationships that could have appeared to influence the work reported in this paper.

Data availability

Data will be made available on request.

Acknowledgements

The authors thank the BISCEM technical platform (Univ. Limoges, Inserm US042, CNRS UAR 2015, CHU Limoges) for providing access to high resolution mass spectrometry equipment, and Dr Yves Champavier for his help with NMR result interpretation.

FDM gratefully acknowledges support from Xavier Montagutelli (University de Limoges, France) for computational and technical support, from the regional supercomputers CALI ("CALcul en Limousin") and "Baba Yaga", as well as from the "Jean-Zay" national supercomputer from IDRIS HPC resources under the allocations 2020-A0080711487, 2021-A0100711487 and 2022-A0120711487 made by GENCI.

Appendix A. Supporting information

Supplementary data associated with this article can be found in the online version at [doi:10.1016/j.phrs.2024.107438](https://doi.org/10.1016/j.phrs.2024.107438).

References

- J.F. Borel, Z.L. Kis, T. Beveridge, The history of the discovery and development of cyclosporine (Sandimmune®), in: V.J. Merluzzi, J. Adams (Eds.), *The Search for Anti-Inflammatory Drugs: Case Histories from Concept to Clinic* [Internet], Birkhäuser Boston, Boston, MA, 1995, pp. 27–63, https://doi.org/10.1007/978-1-4615-9846-6_2.
- H. Ekberg, H. Tedesco-Silva, A. Demirbas, S. Vitko, B. Nashan, A. Gürkan, et al., Reduced exposure to calcineurin inhibitors in renal transplantation, *N. Engl. J. Med.* 357 (25) (2007) 2562–2575.
- J. Miller, J.D. Pirsch, M. Deierhol, F. Vincenti, R.S. Filo, FK 506 in kidney transplantation: results of the U.S.A. randomized comparative phase III study, *Transpl. Proc.* 29 (1–2) (1997) 304–305.
- U. Christians, C. Kruse, R. Kownatzki, H.M. Schiebel, R. Schwinzer, M. Sattler, et al., Measurement of FK 506 by HPLC and isolation and characterization of its metabolites, *Transpl. Proc.* 23 (1 Pt 2) (1991) 940–941.
- K. Iwasaki, T. Shiraga, K. Nagase, Z. Tozuka, K. Noda, S. Sakuma, et al., Isolation, identification, and biological activities of oxidative metabolites of FK506, a potent immunosuppressive macrolide lactone, *Drug Metab. Dispos. Biol. Fate Chem.* 21 (6) (1993) 971–977.
- K. Iwasaki, T. Shiraga, H. Matsuda, K. Nagase, Y. Tokuma, T. Hata, et al., Further metabolism of FK506 (tacrolimus). Identification and biological activities of the metabolites oxidized at multiple sites of FK506, *Drug Metab. Dispos. Biol. Fate Chem.* 23 (1) (1995) 28–34.
- U. Christians, F. Braun, M. Schmidt, N. Kosian, H.M. Schiebel, L. Ernst, et al., Specific and sensitive measurement of FK506 and its metabolites in blood and urine of liver-graft recipients, *Clin. Chem.* 38 (10) (1992) 2025–2032.
- A.K. Gonschior, U. Christians, M. Winkler, A. Linck, J. Baumann, K.F. Sewing, Tacrolimus (FK506) metabolite patterns in blood from liver and kidney transplant patients, *Clin. Chem.* 42 (9) (1996) 1426–1432.
- U. Christians, W. Jacobsen, N. Serkova, L.Z. Benet, C. Vidal, K.F. Sewing, et al., Automated, fast and sensitive quantification of drugs in blood by liquid chromatography-mass spectrometry with on-line extraction: immunosuppressants, *J. Chromatogr. B Biomed. Sci. Appl.* 748 (1) (2000) 41–53.
- I.R. Dubbelboer, A. Pohanka, R. Said, S. Rosenberg, O. Beck, Quantification of tacrolimus and three demethylated metabolites in human whole blood using LC-ESI-MS/MS, *Ther. Drug Monit.* 34 (2) (2012) 134–142.
- M. Shimomura, S. Masuda, M. Goto, T. Katsura, T. Kiuchi, Y. Ogura, et al., Required transient dose escalation of tacrolimus in living-donor liver transplant recipients with high concentrations of a minor metabolite M-II in bile, *Drug Metab. Pharm.* 23 (5) (2008) 313–317.
- K. Tamura, T. Fujimura, K. Iwasaki, S. Sakuma, T. Fujitsu, K. Nakamura, et al., Interaction of tacrolimus(FK506) and its metabolites with FKBP and calcineurin, *Biochem. Biophys. Res. Commun.* 202 (1) (1994) 437–443.
- M. Yanagimachi, T. Naruto, R. Tanoshima, H. Kato, T. Yokosuka, R. Kajiwara, et al., Influence of CYP3A5 and ABCB1 gene polymorphisms on calcineurin inhibitor-related neurotoxicity after hematopoietic stem cell transplantation, *Clin. Transpl.* 24 (6) (2010) 855–861.
- J. Zegarska, E. Hryniewiecka, D. Zochowska, E. Samborowska, R. Jazwiec, A. Borowick, et al., Tacrolimus metabolite M-III may have nephrotoxic and myelotoxic effects and increase the incidence of infections in kidney transplant recipients, *Transpl. Proc.* 48 (5) (2016) 1539–1542.
- J. Zegarska, E. Hryniewiecka, D. Zochowska, E. Samborowska, R. Jazwiec, K. Maciej, et al., Evaluation of the relationship between concentrations of tacrolimus metabolites, 13-O-demethyl tacrolimus and 15-O-demethyl tacrolimus, and clinical and biochemical parameters in kidney transplant recipients, *Transpl. Proc.* 50 (7) (2018) 2235–2239.
- T. van Gelder, A. Gelinck, S. Meziyerh, A.P.J. de Vries, D.J.A.R. Moes, Therapeutic drug monitoring of tacrolimus after kidney transplantation: trough concentration or area under curve-based monitoring? *Br. J. Clin. Pharm.* (2024).
- M.D. Hanwell, D.E. Curtis, D.C. Lonie, T. Vandermeersch, E. Zurek, G.R. Hutchison, Avogadro: an advanced semantic chemical editor, visualization, and analysis platform, *J. Cheminf.* 4 (1) (2012) 17.
- K.P. Wilson, M.M. Yamashita, M.D. Sintchak, S.H. Rotstein, M.A. Murcko, J. Boger, et al., Comparative X-ray structures of the major binding protein for the immunosuppressant FK506 (tacrolimus) in unliganded form and in complex with FK506 and rapamycin, *Acta Crystallogr D Biol. Crystallogr* 51 (4) (1995) 511–521.
- Y. Zhao, D.G. Truhlar, The M06 suite of density functionals for main group thermochemistry, thermochemical kinetics, noncovalent interactions, excited states, and transition elements: two new functionals and systematic testing of four M06-class functionals and 12 other functionals, *Theor. Chem. Acc.* 120 (1–3) (2008) 215–241.
- S.J. Li, J. Wang, L. Ma, C. Lu, J. Wang, J.W. Wu, et al., Cooperative autoinhibition and multi-level activation mechanisms of calcineurin, *Cell Res.* 26 (3) (2016) 336–349.
- J.P. Griffith, J.L. Kim, E.E. Kim, M.D. Sintchak, J.A. Thomson, M.J. Fitzgibbon, et al., X-ray structure of calcineurin inhibited by the immunophilin-immunosuppressant FKBP12-FK506 complex, *Cell* 82 (3) (1995) 507–522.
- Y. Dai, M.F. Hebert, N. Isoherranen, C.L. Davis, C. Marsh, D.D. Shen, et al., Effect of CYP3A5 polymorphism on tacrolimus metabolic clearance in vitro, *Drug Metab. Dispos.* 34 (5) (2006) 836–847.
- K. Iwasaki, Metabolism of Tacrolimus (FK506) and Recent Topics in Clinical Pharmacokinetics, *Drug Metab. Pharm.* 22 (5) (2007) 328–335.
- W. Schöler, P. Schmieder, H. Kessler, U. Christians, I. Holze, K. Sewing, et al., Structural investigations of 13-O-demethyl-FK506 and its isomers generated by *in vitro* metabolism of FK506 using human-liver microsomes, *Helv. Chim. Acta* 76 (6) (1993) 2288–2302.
- I.J. General, H. Meirovitch, Absolute free energy of binding and entropy of the FKBP12-FK506 complex: effects of the force field, *J. Chem. Theory Comput.* 9 (10) (2013) 4609–4619.
- G. Solomentsev, C. Diehl, M. Akke, Conformational entropy of FK506 binding to FKBP12 determined by nuclear magnetic resonance relaxation and molecular dynamics simulations, *Biochemistry* 57 (9) (2018) 1451–1461.
- J. Zou, C. Tian, C. Simmerling, Blinded prediction of protein-ligand binding affinity using Amber thermodynamic integration for the 2018 D3R grand challenge 4, *J. Comput. Aided Mol. Des.* 33 (12) (2019) 1021–1029.
- B.E. Bierer, P.S. Mattila, R.F. Standaert, L.A. Herzenberg, S.J. Burakoff, G. Crabtree, et al., Two distinct signal transmission pathways in T lymphocytes are

- inhibited by complexes formed between an immunophilin and either FK506 or rapamycin, *Proc. Natl. Acad. Sci. USA* 87 (23) (1990) 9231–9235.
- [29] P.R. Juvvadi, D. Fox, B.G. Bobay, M.J. Hoy, S.M.C. Gobeil, R.A. Venters, et al., Harnessing calcineurin-FK506-FKBP12 crystal structures from invasive fungal pathogens to develop antifungal agents, *Nat. Commun.* 10 (1) (2019) 4275.
- [30] K. Tamura, T. Fujimura, K. Iwasaki, S. Sakuma, T. Fujitsu, K. Nakamura, et al., Interaction of tacrolimus(FK506) and its metabolites with FKBP and calcineurin, *Biochem. Biophys. Res. Commun.* 202 (1) (1994) 437–443.